

Membranes fabricated with a deep single corrugation for package stress reduction and residual stress relief

V L Spiering†, S Bouwstra‡, J F Burgert† and M Elwenspoek†

† MESA Research Institute, University of Twente, PO Box 217, 7500 AE Enschede, The Netherlands

‡ Microelectronic Centre (MIC), Technical University of Denmark (DTH), Lyngby, Denmark

Abstract. Thin square membranes including a deep circular corrugation are realized and tested for application in a strain-based pressure sensor. Package-induced stresses are reduced and relief of the residual stress is obtained, resulting in a larger pressure sensitivity and a reduced temperature sensitivity. Finite element method simulations were carried out, showing that the pressure-deflection behaviour of the structure is close to that of a circular membrane with clamped edge but free radial motion.

1. Introduction

Packaging-induced stress is usually an unwanted phenomenon in micromechanical devices [1]. Especially in high sensitivity micromechanical sensors package-stresses can jam the sensor output. These stresses can be reduced by the application of a mechanical decoupling zone [2–4]. In [2] a theoretical model was presented for the mechanical behaviour of a deep circular V-groove as the decoupling zone and it was shown that a very high reduction of stresses is reached for deep, thin zones. Spiering *et al* [4] report on the fabrication of a membrane with an on-chip decoupling zone. In this paper thin square silicon nitride membranes are compared with the same membranes including a deep circular corrugation. The residual stress as well as thermally induced centre deflections are measured.

Figure 1 shows the structures considered: (a) a thin square membrane and (b) the same membrane containing a thin corrugated circular zone. The grooves (front side) were etched into the bulk silicon by reactive ion etching with a SF_6/O_2 plasma and afterwards covered with $1\text{ }\mu\text{m}$ low-pressure chemical vapour deposited (LPCVD) silicon nitride. The backside etching was done in a KOH solution. Figure 2 shows a photograph of the resulting structure.

2. Model

For a flat clamped square membrane with thickness t , length $2a$, Young's modulus E , Poisson's ratio ν and initial stress σ_0 the relation between the pressure

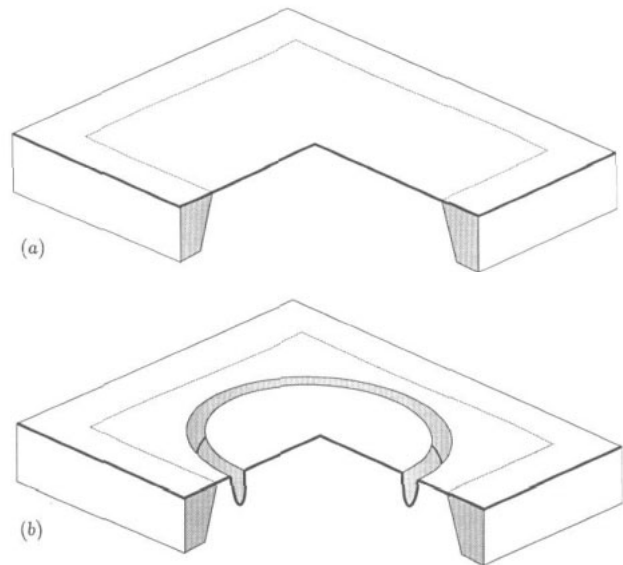


Figure 1. 3D view of the structures considered (a) flat membrane, (b) membrane with a deep circular corrugation for package stress reduction and low residual stress.

difference P over the membrane and the corresponding centre deflection y is [5, 6]:

$$P = \frac{C_1 t \sigma_0}{a^2} y + \frac{C_2 f(\nu) t E}{a^4 (1 - \nu)} y^3. \quad (1)$$

The first term shows the stiffness due to residual stress. The second term shows a flattening out in y for larger pressures as a result of stretching of the membrane. For square membrane $C_1 = 3.41$, $C_2 = 1.98$, and $f(\nu) = 1 - 0.296\nu$ [6].

The membranes including the circular zone were modelled with the finite element method

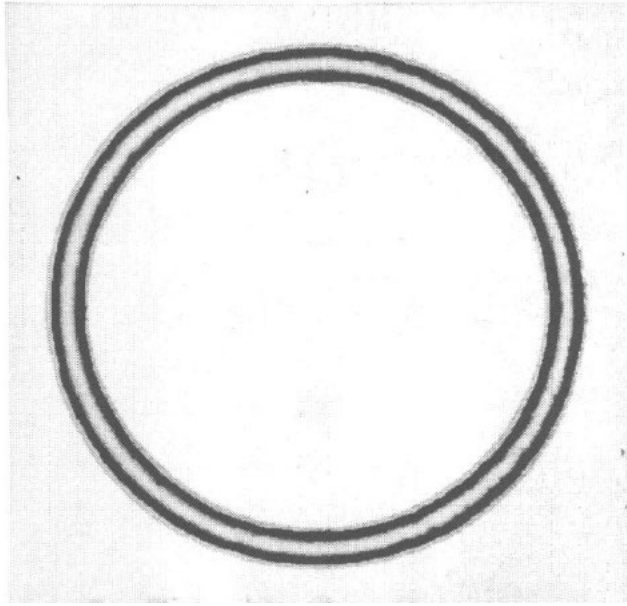


Figure 2. Photograph of a square silicon nitride membrane containing a 100 μm deep corrugation.

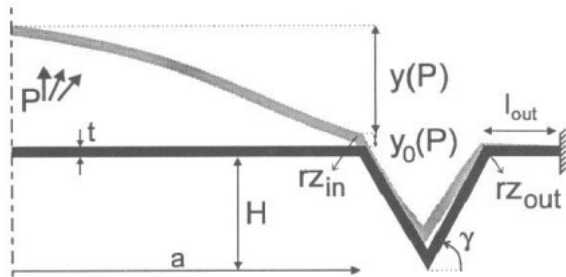


Figure 3. Definitions of parameters of the corrugated structure.

(SYSTUS Framatome software) using axisymmetrical shell elements. Thickness, depth and shape of the corrugation were varied as well as the length of the flat part at the outer edge of the zone. Figure 3 shows the definition of the applied parameters. Note that $y(P)$ denotes the centre deflection minus the (offset) deflection y_0 of the inner edge of the corrugation.

Figure 4 shows the non-linear deflection–pressure curve $y(P)$ for the corrugated structure as well as for several *circular* membranes with radius a under different edge conditions: clamped edge, clamped with free radial motion of the edge, simply supported, and the latter with free radial motion of the edge. All simulations and calculations were done with a zero initial stress, which is close to the real situation for a deep corrugation [2]. A Young's modulus $E = 245 \text{ GPa}$, Poisson's ratio $\nu = 0.3$ and standard dimensions: $t = 1 \mu\text{m}$, $H = 100 \mu\text{m}$, $a = 0.35 \text{ mm}$, $l_{\text{out}} = 50 \mu\text{m}$ and $\gamma = 60^\circ$ were applied. The best description of the mechanical behaviour of the membrane with a corrugated zone is given by the membrane with clamped edges with free radial motion: the zone is weak for radial loads but relatively stiff for the lateral pressure load. Therefore the rotation of the

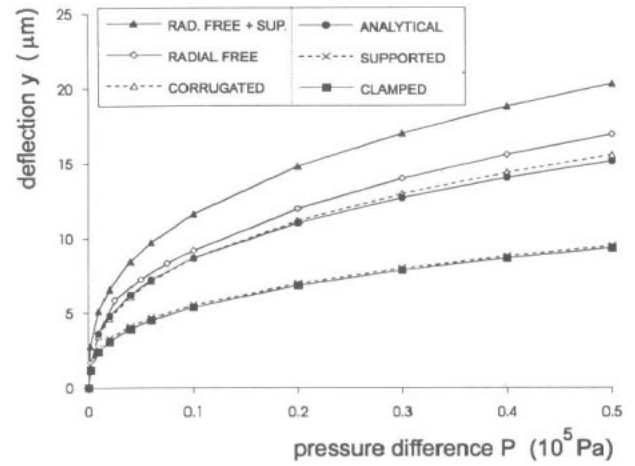


Figure 4. FEM results for the centre-edge deflection as a function of pressure difference for membranes with different edge conditions: clamped, clamped but radially free to move, simply supported, simply supported and radially free to move, and the corrugated structure. Analytical results for a membrane with clamped edge but free radial motion are plotted as well.

edge at the inner radius of the zone can be ignored. The analytical description of this circular membrane with radius a is given by:

$$P = \frac{C_3 E t^3}{a^4} y + \frac{C_4 E t}{a^4 (1 - \nu)} y^3 \quad (2)$$

with a bending coefficient $C_3 = 5.85$ and the non-linear coefficient $C_4 = 0.598$ for $\nu = 0.3$ [7]. A non-linear term is still present, not because of stretching but because of increased stiffness due to the shell shape. This model could be further refined by including a rotational stiffness at the edge, rather than the clamped condition.

Detailed investigation of linear FEM results ($P = 1 \text{ Pa}$) shows that the flat rim outside the corrugation with length l_{out} results in an increasing offset displacement y_0 for increasing l_{out} . This is caused by changes of the deflection and the rotation at the outer radius of the zone. However, the values of deflections and rotations of the actual membrane are not affected. Moreover the effect can be suppressed by choosing l_{out} as small as possible: for $l_{\text{out}} \rightarrow 0$ the offset displacement $y_0 \rightarrow 0$. Also for corrugation depths above 25 μm and zone-angles above 30° the deformation of the membrane is not affected by the actual dimensions of the corrugation, see figure 5. The increase of the deflections and rotations for a zone depth $H = 10 \mu\text{m}$, is explained by the fact that the membrane now approaches the structure of the (larger) square membrane.

3. Experimental results

To test the reduction of stresses, samples were mounted on a steel backplate with a pressure inlet, which was placed on a Peltier element to control the temperature, see figure 6. The temperature was measured with a

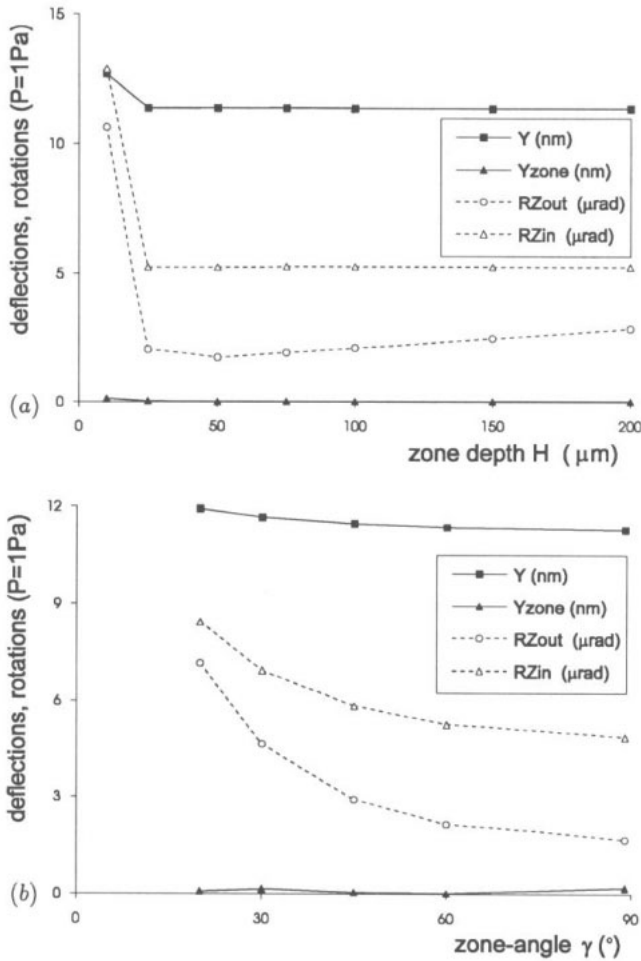


Figure 5. Displacements and rotations of the structure as a function of (a) zone depth H ($\gamma = 60^\circ$), and (b) zone angle ($H = 100 \mu\text{m}$). Y zone denotes the vertical displacement between inner and outer edge of the zone.

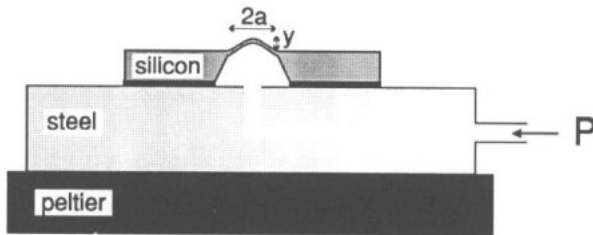


Figure 6. Experimental set-up.

thermocouple located close to the membrane. The pressure was adjusted and measured by a pressure regulator and deflections were recorded by a DEKTAK mechanical profile scanner.

Table 1. Experimental results for (1) a flat membrane and membranes with a corrugation of (2) $25 \mu\text{m}$ and (3) $100 \mu\text{m}$.

Sample	Zone inner radius (μm)	Zone depth (μm)	Zone width (μm)	$E/(1-\nu)$ (GPa)	Initial stress σ_0 (MPa)	$d((Y_{P,T}/Y_{P,T_0}) - 1)/dT$ ($10^{-4}/^\circ\text{C}$)	$d\sigma/dT$ (MPa/ $^\circ\text{C}$)
1 (\square)	-	-	-	350	85	-100	5.5
2	386	25	75	375 ^a	< 10	- 3.38	< 0.05
3	355	100	150	375 ^a	< 10	- 2.53	< 0.05

^a Measured from a square membrane on the same wafer.

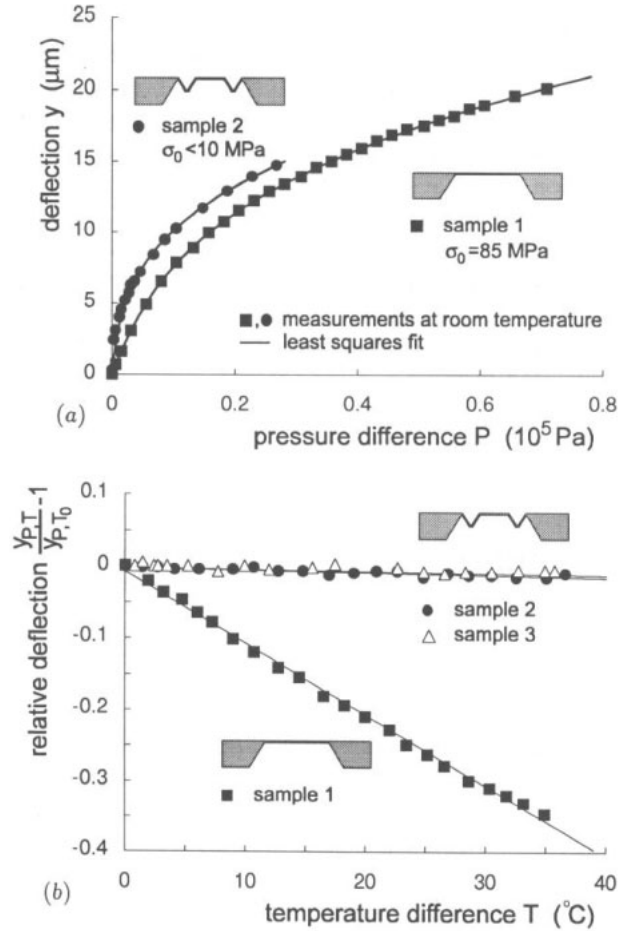


Figure 7. (a) Pressure-deflection measurements and least squares fit to model both membrane structures at room temperature, and (b) the relative change of deflection at constant pressure (30 kPa) as a function of temperature elevation for the membrane structures.

Figure 7(a) shows the pressure-deflection measurements of a $1 \times 1 \text{ mm}$ silicon-nitride membrane with thickness of $1 \mu\text{m}$ as well as a membrane with the same dimensions containing a zone with dimensions as given in table 1. The bi-axial elasticity modulus $E/(1-\nu)$ differed a little between the samples and an initial stress $\sigma_0 = 85 \text{ MPa}$ was found for the flat membrane. Due to the very low initial stress the pressure-deflection curve of the membrane with zone has a very small linear part over the pressure range considered. Although this makes a reliable fitting of the measured curve difficult, it can be concluded that the residual stress σ_0 was at least reduced to 10 MPa .

Heating the sample with a Peltier element results in an additional thermal (package) stress. The centre deflection y was monitored at constant pressure as a function of the temperature, see figure 7(b). The deflections $y_{P,T}$ were normalized with respect to the deflection y_{P,T_0} at room temperature. For the flat membrane a thermal sensitivity of the total residual stress $d\sigma/dT = 5.5 \text{ MPa/}^\circ\text{C}$ was determined, using the pressure-deflection test. The measurements on membranes containing a decoupling zone show a large reduction of the thermal influence. The results are summarized in table 1.

4. Conclusions

Thin membranes including a deep single circular corrugation have been realized and characterized by means of their pressure-deflection behaviour. Package-induced and thermal stresses are reduced while a relief of the residual stress is obtained in the inner circular membrane. FEM simulations showed that the deformation of the inner membrane is hardly affected by the actual dimensions of the corrugation. A good estimate of this deformation is given by a circular membrane with clamped edge but free motion in the radial direction.

The increasing pressure sensitivity and the decreasing temperature sensitivity make the membranes including the circular corrugation very attractive for application in strain based pressure sensors.

Acknowledgments

These investigations in the programme of the Foundation for Fundamental Research on Matter (FOM) have been supported by the Netherlands Technology Foundation (STW).

References

- [1] Senturia S D and Smith R L 1988 Microsensor packaging and system partitioning *Sens. Actuators* **15** 221-34
- [2] Spiering V L, Bouwstra S, Spiering R M E J and Elwenspoek M 1991 On-chip decoupling zone for package-stress reduction *Sens. Actuators* **A39** 149-56
- [3] Offereins H L, Sandmaier H, Folkner B, Steger U and Lang W 1991 Stress-free assembly technique for a silicon based pressure sensor *Proc. 6th Int. Conf. Solid-State Sensors and Actuators (San Francisco, CA, 1991)* (New York: IEEE) pp 985-9
- [4] Spiering V L, Bouwstra S and Fluitman J H J 1993 Realization of decoupling zones for package-stress reduction *Sens. Actuators* **A37-38** 800-4
- [5] Tabata O, Kawahata K, Sugiyama S and Igarashi I 1989 Mechanical property measurements of thin films using load-deflection of composite rectangular membranes *Sens. Actuators* **20** 135-41
- [6] Pan J Y, Lin P, Maseeh F and Senturia S D 1990 Verification of FEM analysis of load-deflection methods for measuring mechanical properties of thin films *IEEE Solid-State Sensor and Actuator Workshop (Hilton Head, SC, 1990)* (New York: IEEE) Technical digest pp 70-3
- [7] Timoshenko S and Woinowsky-Krieger S 1970 *Theory of Plates and Shells* 2nd edn (New York: McGraw-Hill) pp 396-412